Energy 188 (2019) 116025

Contents lists available at ScienceDirect

Energy

journal homepage: www.elsevier.com/locate/energy

Optimal parameter identification of triple-junction photovoltaic panel based on enhanced moth search algorithm

Ahmed Fathy [a, b], Mohamed Abd Elaziz [c], Enas Taha Sayed [d, e], A.G. Olabi [f, g, *], Hegazy Rezk [h, i, **]

[a] Electrical Engineering Department, Faculty of Engineering, Jouf University, Saudi Arabia
[b] Electrical Power and Machine Department, Faculty of Engineering, Zagazig University, Egypt
[c] Department of Mathematics, Faculty of Science, Zagazig University, Zagazig, Egypt
[d] Center for Advanced Materials Research, University of Sharjah, PO Box 27272, Sharjah, United Arab Emirates
[e] Chemical Engineering Department, Minia University, Elminia, Egypt
[f] Dept. of Sustainable and Renewable Energy Engineering, University of Sharjah, P.O. Box 27272, Sharjah, United Arab Emirates
[g] Mechanical Engineering and Design, Aston University, School of Engineering and Applied Science, Aston Triangle, Birmingham, B4 7ET, UK
[h] College of Engineering at Wadi Addawaser, Prince Sattam Bin Abdulaziz University, Saudi Arabia
[i] Electrical Engineering Department, Faculty of Engineering, Minia University, Egypt

A R T I C L E I N F O

Article history:
Received 10 February 2019
Received in revised form
25 August 2019
Accepted 26 August 2019
Available online 27 August 2019

Keywords:
Triple-junction solar cell
Moth search algorithm
Disruptor operator

A B S T R A C T

The paper proposes an enhanced moth search algorithm (EMSA) employed in identifying the optimal parameters of Triple-Junction (TJS) photovoltaic panel under different operating conditions. Disruptor operator (DO) is placed in the moth search algorithm (MSA) to improve its performance. The DO is used to improve the diversity of the MSA and avoid it from stuck in local point. The presented fitness function in this work is the integral time absolute error (ITAE) between the triple junction PV panel experimental and calculated currents. The panel is simulated in Simulink and tested under different solar radiation conditions. Additionally, the panel performance is investigated under the shadow effect; a comparative study is performed with other metaheuristic optimization approaches and with Hammerstein and wiener identification technique. The proposed EMSA operates with efficiencies around 99.66% and 99.89%for first and second patterns respectively. It is confirmed the superiority and reliability of the proposed EMSA in extracting the optimal parameters of TJS based module operated at different operating conditions.

1. Introduction

With ever dwindling natural resources and increasing demands for power, the need to seek out viable alternative sources of renewable energy is not just acute but urgent. Recently, photovoltaic (PV) conversion gains great attention as a green energy source and available in a massive amount as well. PV system (PVS) is considered as one of the most promising technologies of renewable energies because it is clean, noise-free, and friendly to the environment with the comparison to conventional sources such as based on fossil fuels [1–3]. In recent years, the multi-junction solar cells (MJSC) have more attention since they are used on concentrated PV systems that can produce electrical power at a lower cost of energy than the traditional flat-plate PVSs. The structure of the MJSC contains three sub-cells, which are connected in series using the tunnel junctions. This gives the MJSC high ability to convert a large amount of sunlight into energy at high efficiency. According to these properties; the MJSC has been used in space and terrestrial applications that require low and high concentrations, respectively. The GaInP/GaInAs/Ge triple-junction solar cell (TJSC) is considered as one of the most popular MJSC types; it can reach efficiency of 46% [4]. Combined tables clarifying a general list of the highest efficiencies for solar cells and modules have been presented by *Green* et al., [5]. However, the performance of cells depends on the temperature and concentration; therefore; there are several

* Corresponding author. Dept. of Sustainable and Renewable Energy Engineering, University of Sharjah, P.O. Box 27272, Sharjah, United Arab Emirates.
** Corresponding author. College of Engineering at Wadi Addawaser, Prince Sattam Bin Abdulaziz University, Saudi Arabia.
E-mail addresses: aolabi@sharjah.ac.ae (A.G. Olabi), hegazy.hussien@mu.edu.eg (H. Rezk).

https://doi.org/10.1016/j.energy.2019.116025
0360-5442/

models that have been presented to define these parameters. For example, *Kinsey* et al. [6], proposed semi-empirical cell to predict the performance of the cell by representing the performance as a function of temperature and solar concentration. *Reinhardt* et al. [7], proposed two diodes equivalent circuit (TDEC) model, which evaluated at 1-sun and room temperature against the InGaP/InGaAs/Ge cell data. *Nishioka* et al. [8] evaluated the TDEC model at concentration variant from 1 to 1000 W/m^2 and at room temperature. However, in the two models, high concentration and cell temperature are frequently encountered during the actual work of the cell, and thus, it is vital to study them. The authors in Refs. [8,9], proposed a single diode equivalent circuit model which has been evaluated at high concentration and temperature levels. The predictions of this model are calibrated against the sharp cell data [10], which optimizing the coefficient to fit the measured efficiency as current-voltage data was not available. The results of this model refer to the dispersion of the predictions of efficiency-temperature coefficients and open circuit voltage at high concentrations from the data is high. *Segev* et al. [11], proposed single and two diodes equivalent circuits based on semi-empirical models for InGaP/InGaAs/Ge Triple-Junction cells, calibrated against available empirical data published by two cell manufacturers. *Das* et al., [12] presented a model for the MJSC based on MATLAB/Simulink software to enhance the conversion efficiency. In this model, the multi-junction and conventional silicon photovoltaic (PV) cells are compared, and the results indicate that triple-junction solar cell improves its maximum power three times than the maximum power of the conventional one.

In all modules mentioned above, several operating parameters such as short circuit current, open circuit voltage, voltage and current at maximum power point (MPP), power at MPP, and the temperature coefficients of current and voltage are provided by the manufactures (single-junction PV module manufacturer's datasheet). However, an additional set of other parameters are not included in the PV module manufacturer's datasheet such as saturation current, parallel resistance, photon current, series resistance, and ideality factor of diode parameters. Therefore, there are several methods have been proposed for the identification of these parameters. For example, Newton Raphson method is used to determine the optimal value for the seven parameters [13]. Also, *Elbaset* et al., [14], presented the Newton Raphson and Runge–Kutta Merson iteration methods to evaluate the performance of the model to fit non-linear output characteristics of *P–V* and *I–V*. *Patra* et al. [15], proposed a model for MJSC characterization which contains eight parameters, where three of them used to describe the voltage-current characteristic in negative voltage and the other parameters in a positive one as well as, the Lambert W-function is used to find the optimal value for the parameters of TJSCs at uniform irradiation and temperature. Moreover, there are several metaheuristic methods have been applied to determine the optimal parameters of the single junction solar cell (SJSC). The common and widely adopted mathematical models of SJSC are the single-diode model and the double-diode model. For example, generalized oppositional teaching-learning based [16], harmony search [17], simulated annealing based on Levenberg–Marquardt method [18], cat swarm optimization [19], chaotic whale optimization algorithm [20], adaptive differential evolution [21], pattern search [22], Chaotic ABC [23], chaos particle swarm algorithm [24]. Zagrouba et al. [25] applied Genetic Algorithm (GA) to identify the optimal parameters of multi-crystalline silicon SC and 50-Watt solar panel. The optimal solution for determination the parameters of single-diode SC is achieved after five whereas after seven iterations for solar panel. The main finding also confirmed that mutation control parameter value must be between 1% and 20% to avoid the convergence to local solution. Similar to the work done by of Zagrouba et al. [25] and Ismail et al. [26] employed GA to determine the optimal parameters of single-double and double-diode models of solar cell. These parameters include series resistance, shunt resistance and diode ideality factor. The main finding confirmed that the most accurate fit obtained by single-diode model. Yu et al. suggested a performance-guided JAYA algorithm to identify the parameters of single-junction solar cell [27]. The parameters estimation performance of the proposed strategy has been tested through three widely used standard datasets of different PV models including single diode, double diode, and PV module. The drawback of this study is neglecting partial shading condition. Both works done by Yu et al. [27] and Zagrouba et al. [25] neglected the partial shading condition. Whereas this condition has been considered by Ismail et al. [26] and Fathy and Rezk [28]. Fathy and Rezk employed imperialist competitive algorithm to solve the parameter estimation problem of PVS [28]. The PVS is modeled using single-diode and double-diode models. The proposed constrained objective function has been extracted from the voltage-power graph of the PVS that has only maximum power point. The analysis is carried out on three types of PV panels; mono-crystalline, poly-crystalline and amorphous modules. Oliva et al. proposed a chaotic improved artificial bee colony optimization algorithm for parameter estimation of single junction solar cells [23]. Single-diode and double-diode models are used in the validation process. The partial shading condition is also ignored in their study. However, there are few works performed on TJSCs using metaheuristic algorithms such as in Ref. [29], which used the water cycle algorithm. In Ref. [30], the series resistance of InGaP/InGaAs/Ge TJSC has been evaluated. *Tsai* et al. [31] presented a general model of PV based on Matlab/Simulink.

Although the merits of the various modern optimizers in the literature, it has been demonstrated that none of these optimizers can solve all optimization problems. This reveals the importance of new algorithms in different fields because the effectiveness of an algorithm in solving a set of problems does not guarantee its success in different sets of test problems. In the same context, the Moth Search Algorithm (MSA) is presented in Ref. [32] as a meta-heuristic algorithm, which simulates the phototaxis and Lévy flights of moths. In general, the moth's movement towards, or away from, the source of light is represented by using the phototaxis. Whereas, the behaviors of the moths can be represented by using the Levy flights, as mentioned in Ref. [32]. In the MSA, the source of light is considered as the best solution. Also, the nearest moths to the best solution used the Lévy flights to represent the flying process around their positions.

Meanwhile, the other moths, those far away from the best moth, will fly directly toward the best solution in a straight line using the phototaxis.

According to these characteristics, the MSA algorithm has been applied to solve a different problem; for example, the global optimization problem [32]. In Ref. [33], the binary version of MSA is used to solve the discounted {0- triple-junction } knapsack problem. However, the MSA still suffers from some drawbacks such as; it can easily be stuck in local solution and slow convergence. These drawbacks result from its exploitation ability that is not as good as its exploration ability. Therefore, this motivated the authors to improve the performance of the MSA by adding the disruptor operator. This operator can enhance the diversity of the traditional MSA, avoiding it from falling in local point. To the best our knowledge, the MSA did not utilize in the field of parameter identification of solar cell yet. Thus, the proposed enhanced moth search algorithm (EMSA) is used for identifying the optimal parameters of Triple-Junction solar-based module. The triple junction model is considered in the present study since the photovoltaic panels based on triple junction solar cell is promising. For example, the GaInP/GaInAs/Ge triple-junction solar cell is considered as one of the most popular triple junction solar cell types; it has high efficiency compared to single junction solar cell. In the proposed methodology, EMSA starts by generating a set of moths (solutions), and then the quality of each moth is evaluated using an objective function. In this work, the objective function is represented by the integral time absolute error (ITAE) between the module experimental and calculated currents. After that, the solutions are updated using the operators of traditional MSA (i.e., phototaxis and Lévy flights). Then the DO is used to update the solutions. The previous steps are repeated until reaching the stop conditions. The obtained results are compared with traditional MSA and other approaches; grey wolf optimizer (GWO), the whale optimization algorithm (WOA) and water cycle algorithm (WCA). To evaluate the quality of the proposed EMSA to estimate the parameters of Triple-Junction solar, the performance of each algorithm is measured via some statistical parameters such as relative error; root mean square error and efficiency.

The rest of this paper is organized as the following: Section 2 presents the basic definition of the Model of Triple-Junction Solar Cell. Section 3 and Section 4 present the Moth Search Algorithm and Disruption operator, respectively. In Section 5, the Proposed Enhanced Moth Search Algorithm is introduced. Section 6 presents the Numerical Analysis. In Section 7, the conclusion and future works are given.

2. Model of Triple-junction solar cell

The equivalent circuit of InGaP/InGaAs/Ge is shown in Fig. 1, it consists of three sub-cells, top, medium, and bottom. The energy gaps are decreased from top to bottom. The current extracted from the solar cell can be calculated as follows:

$$I_C = I_{Li} - I_{Di} - I_{shunti} \quad \forall i = [1,2,3] \tag{1}$$

The light generated current can be expressed as follows:

$$I_{L_i} = GK_C\left[I_{sc_i} + a\left(T - T_{Ref}\right)\right] \tag{2}$$

where T_{Ref} is the reference temperature in °C, a is the short circuit current temperature coefficient in A/°C, K_C is the concentration ratio, and G is the solar radiation W/m^2. The current, voltage drop, and saturation current of the diode are given as follows:

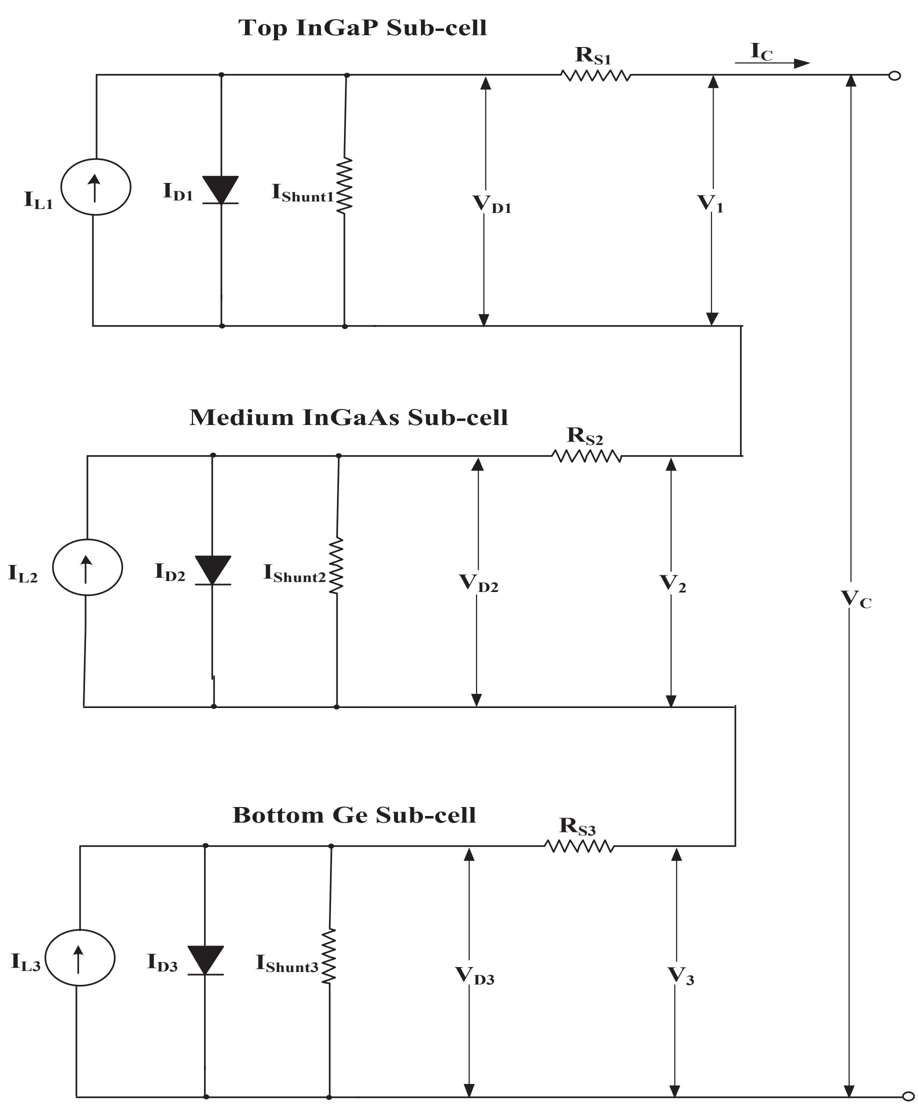

Fig. 1. Configuration of Triple-Junction solar cell.

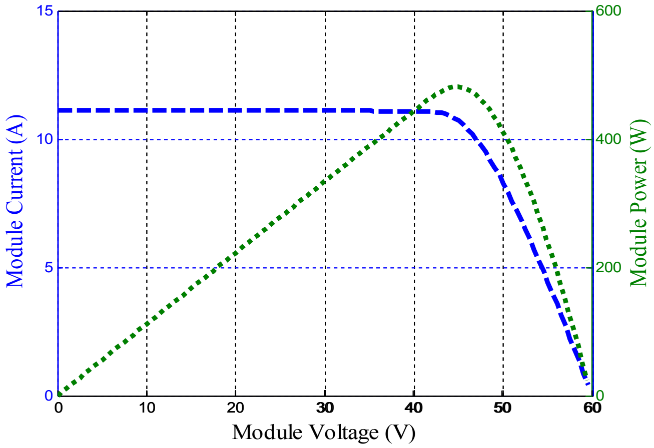

Fig. 2. Current-voltage and power-voltage curves of Triple-Junction solar based module.

$$I_{Di} = I_{Oi}\left[\exp\left(\frac{qV_{Di}}{A_i K_B T}\right) - 1\right] \tag{3a}$$

$$V_{Di} = V_i + I_C \times R_{Si} \tag{3b}$$

$$I_{Oi} = K_i \times T^{\left(3+\gamma/2\right)}\left[\exp\left(-\frac{E_{gi}}{A_i K_B T}\right)\right] \quad \forall i = [1,2,3] \tag{3c}$$

where q is the charge of the electron, A_i is the diode ideality factor, K_B is the Boltzmann's constant, E_g is the energy of bandgap, K and γ are constants, T is the absolute temperature, and R_S is the series resistance of the cell.

The terminal voltage of the Triple-Junction solar cell can be expressed as follows:

$$V_C = \frac{n_1 K_B T}{q}\ln\left[\frac{I_{L1} - I_C}{I_{O1}} + 1\right] + \frac{n_2 K_B T}{q}\ln\left[\frac{I_{L2} - I_C}{I_{O2}} + 1\right] + \frac{n_3 K_B T}{q}\ln\left[\frac{I_{L3} - I_C}{I_{O3}} + 1\right] - I_C \times R_S \tag{4}$$

where;

$$R_S = R_{S1} + R_{S2} + R_{S3} \tag{5}$$

The current-voltage and voltage power curves of Triple-Junction solar-based module are shown in Fig. 2.

3. Overview of moth search algorithm

In this section, the basic information about the traditional moth search algorithm (MSA) is introduced. It is based on the simulation of the behavior of the moths to search for the source of light [32]. The phototaxis and Levy flights are used to represents the exploration and exploitation in MSA. The objective is searching about the light source, so, the moths that have a small distance to the source (the best position of moth) will move around it using the strategy of Levy flights as follows:

$$x_i = x_i + \frac{S_{\max}}{t^2} L(S) \tag{6}$$

where x_i and $S_{\max}$ are the positions of ith moth, and the maximum walk step, respectively, $L(S)$ is the step generated using Levy flights, and it is defined as:

$$L(S) = \frac{(\beta-1)\Gamma(\beta-1)}{\pi S^{\beta}}\sin\left(\frac{\pi(\beta-1)}{2}\right), \quad S \geq 0 \tag{7}$$

where β is Levy distribution's parameter (it is set to 1.5) [29], and Γ is the gamma function. The longest distance moths from the light source will fly toward it directly in line path to update their positions using the following eqn.:

Algorithm 1: Moth search algorithm (MSA) [32]
1. Input: population size N, the dimension dim, the maximum number of iterations t_{max}
2. Determine the initial value for the parameters S_{max}, β, and acceleration factor ω
3. Constructing a random population $X \in R^{N\times dim}$
4. Evaluate each moth (solution) $x_i \in X\ (i = 1,2,\ldots,N)$ using the fitness function.
5. Repeat
6. Sort X according to the fitness function values
7. Divided X into two halves (X_f and X_s) according to fitness function values
8. For each solution in X_f
9. Update $x_i \in X_f$ using eqn. 6
10.Calculate the fitness function of x_i
11.End For
12.For each solution in X_s
13.Update $x_i \in X_s$ using eqn. 8
14.Calculate the fitness function of x_i
15.End For
16.t=t+1
17.Return the best solution x_s

Fig. 3. Pseudo code of moth search algorithm.

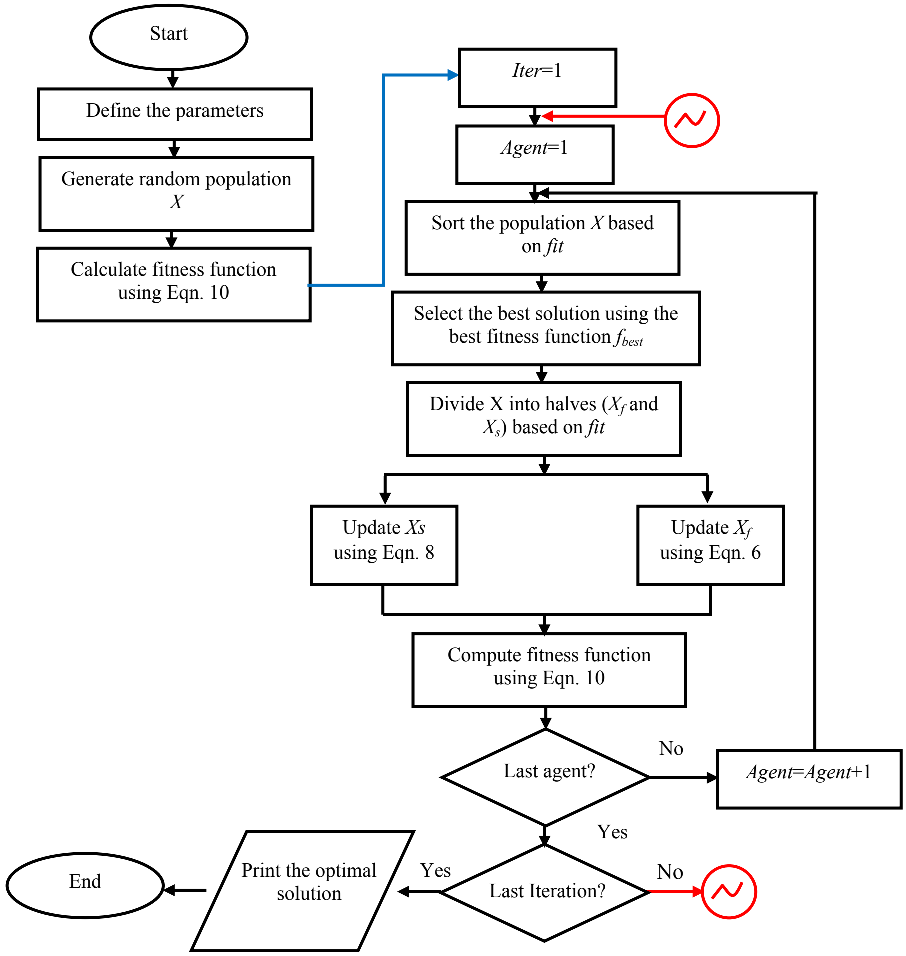

Fig. 4. The proposed solution methodology.

$$x_i = \begin{cases} \gamma(x_i + \omega \times (x_s - x_i)) & \Pr \leq 0.5 \\ \gamma\left(x_i + \frac{1}{\omega} \times (x_s - x_i)\right) & otherwise \end{cases} \quad (8)$$

where ω and x_s represent the acceleration factor and the best moth, respectively. The Pseudo code of moth search algorithm is given in Fig. 3.

4. Disruption operator concept

Disruption operator simulates the astrophysics phenomenon which states that; in the case of the gravitationally bound particles set which have mass m is closed to object with mass M, then this set of particles becomes a torn apart. Like that, in the case of the solid bodies, which held together by using gravitational forces, approaches a much more massive object. The definition of the disruption operator is formulated as follows [34]:

Table 1
Optimal parameters obtained by EMSA compared with others.

Parameter	GWO	WOA	WCA [23]	MSA	GA	PSO	Hybrid PSOGWO	Proposed EMSA
Experiment MPP (W)	571.2143							
Model MPP (W)	570.7732	569.1317	567.21	568.2924	564.3857	570.1003	570.0896	570.9369
A_1	1.950	1.9657	1.9816	1.9787	1.9738	2.0365	1.9741	1.9917
A_2	1.7587	1.99882	1.72	1.9252	1.7312	1.6257	1.7236	1.9220
A_3	2.000	1.93365	1.9798	1.9999	1.9414	2.6453	1.9775	1.9788
R_s (Ω)	0.0206	0.02011	0.0206	0.0204	0.0206	0.0202	0.0206	0.0206
I_{o1} (A)	2.989e-14	2.976e-14	2.989e-14	2.989e-14	2.97e-14	2.90e-14	2.97e-14	2.9896e-14
I_{o2} (A)	2.559e-11	2.446e-11	2.60e-11	2.61e-11	2.57e-11	3.14e-11	2.399e-11	2.56539e-11
I_{o3} (A)	6.175	6.260998	6.3268	6.1802	6.4110	6.3729	6.533	6.1750
I_{L1} (A)	0.0139	0.013892	0.013869	0.0139	0.0139	0.0138	0.0139	0.0139
I_{L2} (A)	0.0149	0.01490	0.0149	0.0149	0.0149	0.0147	0.0149	0.0149
I_{L3} (A)	0.02019	0.02019	0.02057	0.0202	0.0210	0.0206	0.0202	0.0202
ITAE (A)	0.022867	0.0227271	0.020506	0.017209	0.023008	0.0224	0.0233	0.014261

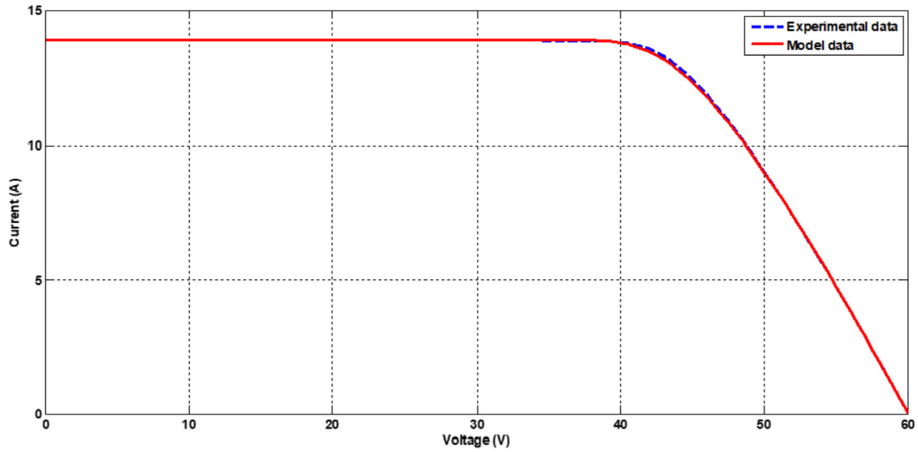

Fig. 5. Current-voltage curve for the experimental and calculated model.

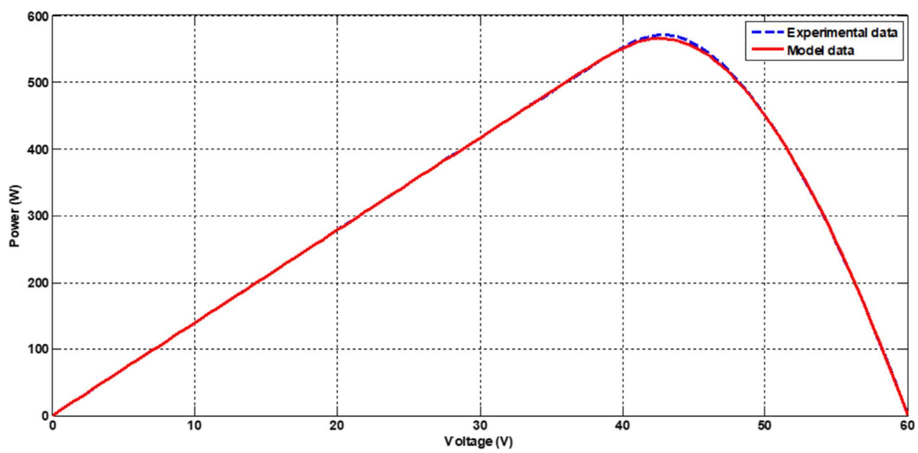

Fig. 6. Power-voltage curve for the experimental and calculated model.

Table 2
Statistical parameters of EMSA compared with GWO, WOA, WCA, MSA, GA, PSO and hybrid PSOGWO approaches.

Parameter		GWO	WOA	WCA [23]	MSA	GA	PSO	Hybrid PSOGWO	Proposed EMSA
Best		0.022867	0.0227271	0.020506	0.017209	0.023008	0.0224	0.0233	0.014261
Worst		0.0849	0.31732	0.0269	0.093445	0.06036	0.15574	0.5141	0.042335
Mean		0.0243	0.02791	0.02066	0.019635	0.0356	0.041478	0.0489	0.017526
Median		0.0232	0.025119	0.020506	0.017673	0.0329	0.034175	0.0359	0.018073
Std. dev.		0.0070	0.029999	0.00792	0.008509	0.0116	0.030364	0.0504	0.0032
RE		1.183401	1.546606	0.974546	1.426347	1.209	0.818	1.2501	0.908805
RMS		2.740029	0.861711	2.347791	0.426347	2.8322	0.455	3.1657	0.07832
Efficiency (ξ)		99.922%	99.635%	99.299%	99.49%	98.805%	99.805%	99.803%	99.951%
Kruskal Wallis test	*p*-value	0.5361	1.066e-05	0.9878	9.172e-06	0.8959	0.9854	0.6010	9.0128e-06
Null hypothesis at 1% significance level		Accept	Reject	Accept	Reject	Accept	Accept	Accept	Reject
Wilcoxon test	*p*-value	0.0143	0.7297	0.8990	3.28e-05	0.2665	0.7638	0.6620	2.9028e-06
	h	1.0	0.0	0.0	1.0	0.0	0.0	0.0	1.0
Null hypothesis of zero median		Reject	Accept	Accept	Reject	Accept	Accept	Accept	Reject
Holm-Bonferroni	*p*-value	0.0858	2.6480	1.5276	0.0002	1.3325	2.1891	2.6480	2.322e-05
Correction test	*h*	0	0	0	1	0	0	0	1
	Significant	×	×	×	✓	×	×	×	✓

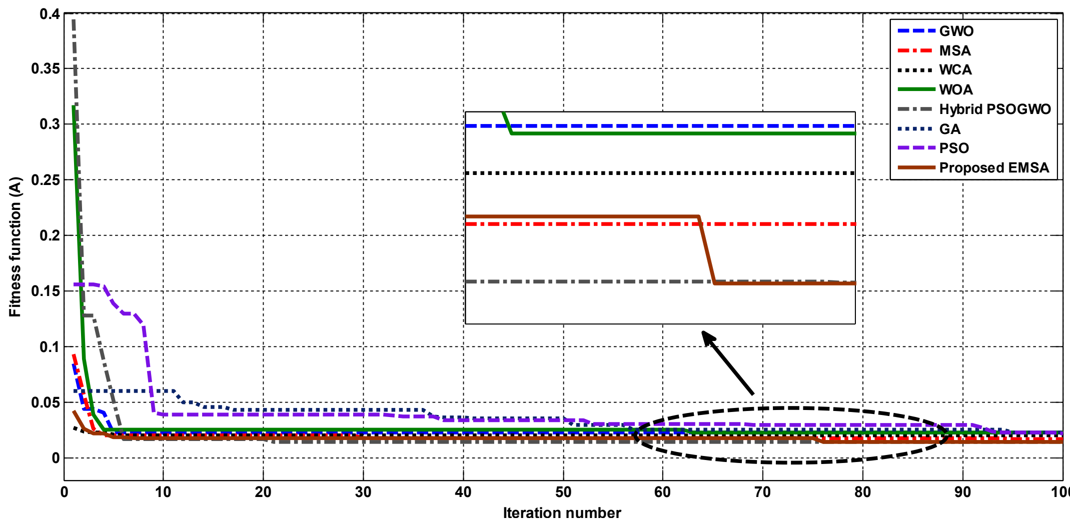

Fig. 7. Variation of fitness function with iteration number at STC.

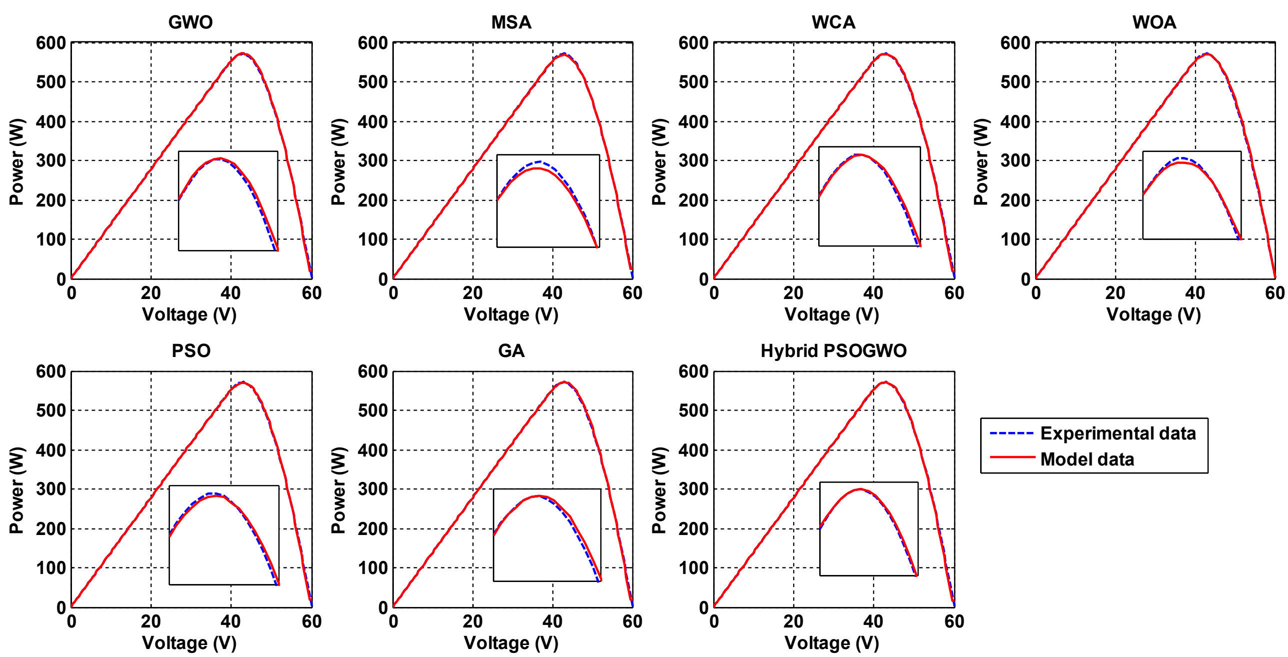

Fig. 8. Power-voltage curves for GWO, WOA, WCA, MSA, GA, PSO, and hybrid PSOGWO.

$$DO = \begin{cases} D_{ij} \times \theta\left(\frac{-1}{2}, \frac{1}{2}\right) & D_{is} \geq 1 \\ 1 + D_{is} \times \theta\left(\frac{-10^{16}}{2}, \frac{10^{16}}{2}\right) & Otherwise \end{cases} \tag{9}$$

where D_{ij} represents the Euclidean distance between ith moth and the nearest neighborhood moth j. While D_{is} is the distance between the i th moth and the best solution and $\theta\,(a, b)$ is a random uniform number generated in the interval [a, b].

5. Proposed enhanced moth search algorithm

In this section, the proposed algorithm to determine the parameters of Triple-Junction solar based module is presented. The variables to be determined are ideality factor (A_i), reverse saturation current (I_{oi}), lighting current (I_{Li}) of each sub-cell, and series resistance of the cell (R_s). The proposed strategy attempts to find the optimal values for the variables mentioned above such that obtaining characteristics that closely matched with experimental curves via minimizing the integral time absolute error (ITAE) between the experimental and calculated model currents. The proposed algorithm combines traditional MSA with disruptor operator. The aim of using the disruptor operator is to improve the diversity of the MSA and avoid it from falling in local point. The proposed EMSA starts by building a random population with size N and

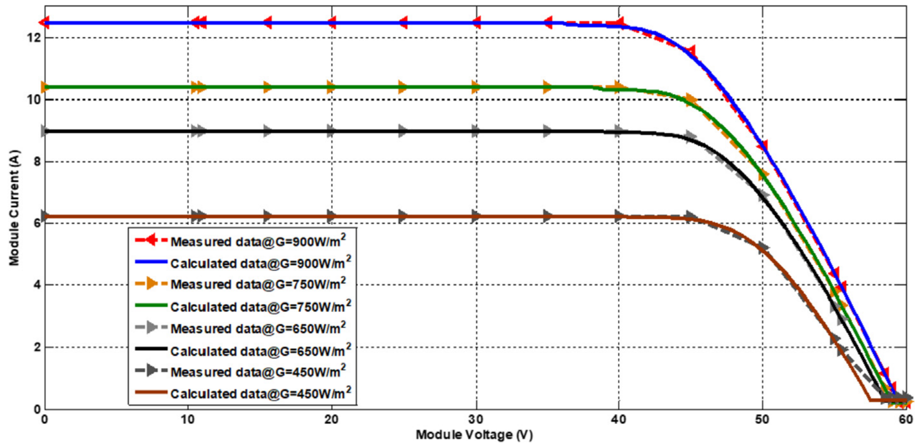

Fig. 9. Current-voltage curves for TJS based module operated under different solar radiations.

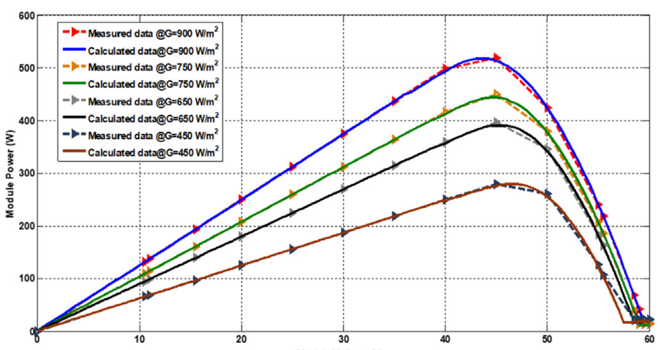

Fig. 10. Power-voltage curves for TJS based module operated under different solar radiations.

Table 3
Statistical parameters of EMSA for TJS based module operated under different solar radiations.

Solar radiation	900 W/m^2	750 W/m^2	650 W/m^2	450 W/m^2
Best	0.018565	0.0139	0.0112	0.012645
Worst	0.0323	0.0279	0.0425	0.047075
Mean	0.0206	0.0152	0.0139	0.019003
Median	0.0186	0.0139	0.0112	0.012645
Std. dev.	0.0056	0.0039	0.0083	0.011674

dimension *dim*. Then for each solution in X; the fitness function is computed as in the following eqn.:

$$fit = \int_{k=1}^{k=m} k.\left(\left| I_M(k) - \sum_{i=1}^{3}\left(GK_C\left[I_{SCi} + \alpha\left(T - T_{ref}\right)\right] - K_i \times T^{\left(3+\gamma_i/2\right)}\left[\exp\left(-\frac{E_{gi}}{A_i K_B T}\right)\right] - I_{Shi}\right)\right|\right) \quad dk \tag{10}$$

The next step is to sort the solutions in X according to the values of the fitness function and determine the best solution (x_s). After that, the population X is divided into two halves (X_f and $X_{s,}$ which represent the first and second halves, respectively) in which the solutions inside each half will be updated using different strates. The solution in the second half X_s is updated using equation (8) that represents flying in a straight line toward the source of light (x_s). Meanwhile, the solutions belong to X_f are updated through using the Levy flights strategy. After that, the solution is updated using the disruptor operator as described in the following eqn.:

$$X = X \odot DO \tag{11}$$

where $\odot$ means the element-wise multiplications, the previous steps are repeated until the maximum iterations and number of agents are met. The general framework of the proposed algorithm is given in Fig. 4.

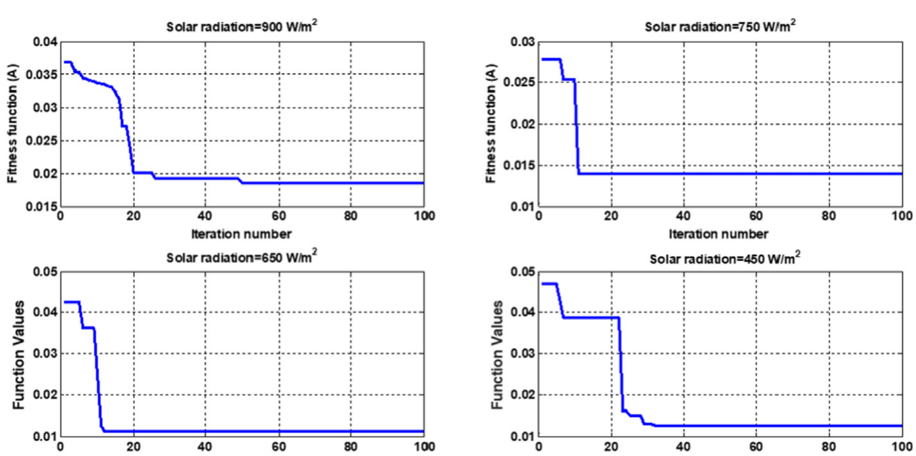

Fig. 11. Fitness function versus iteration number obtained via EMSA at different solar radiations.

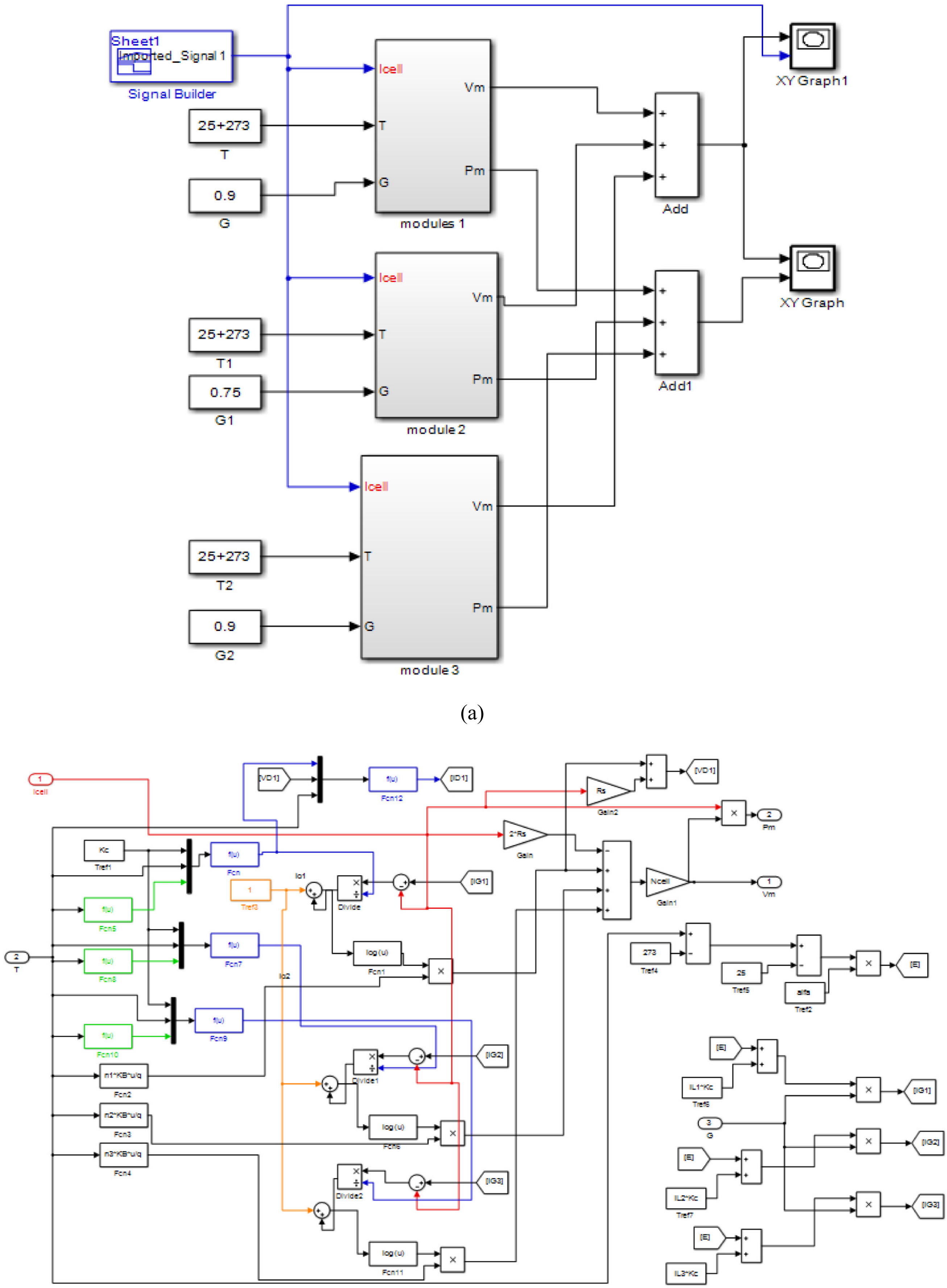

Fig. 12. (a) TJS based array, (b) TJS based module.

6. Numerical Analysis

The analysis is performed on Triple-Junction solar based module with electrical specifications given in Ref. [21]. The controlling parameters of the proposed EMSA are selected as the number of iterations is 100, the number of agents is 50, and the maximum step size (S_{max}) is 0.009. It is assumed that the module is operated at STC ($G = 1000\ W/m^2$ and $T = 298\ K$). The proposed EMSA is implemented, and the obtained results shown in Table 1 are compared with other heuristic algorithms, grey wolf optimizer, the whale optimization algorithm, water cycle algorithm, traditional moth MSA, GA, PS, and hybrid PSOGWO. The experimental global maximum power is 571.2143 W; the proposed approach succeeded in obtaining 570.9369 W as GMPP, which is the best one compared to the others. Additionally, it is clear that the minimum fitness function is 0.014261 A obtained via the proposed EMSA. The current-voltage and power-voltage curves of the experimental and calculated models are shown in Figs. 5 and 6 which confirm the remarkably matching between them.

The performance of each algorithm is measured via statistical parameters, which are best, worst, mean, median, standard deviation, relative error (RE), and root mean square error (RMSE). Additionally, the approach efficiency (ζ) is also calculated; all the parameters are tabulated in Table 2; some of these parameters are calculated as follows:

$$RE = \frac{\sum_{k=1}^{m} P_{PVe}(k) - P_{PVt}(k)}{P_{PVt}},$$
$$RMSE = \sqrt{\frac{\sum_{k=1}^{m} \left(P_{PVe}(k) - P_{PVt}(k)\right)^2}{m}}, \tag{12}$$
$$\%\xi = \left(\frac{P_{PVe}}{P_{PVt}}\right)*100$$

where P_{PVe} is the estimated PV power, P_{PVt} is the true PV power, and m is the number of collected data. Both RMSE and RE serve to collect the error' magnitudes in predictions for various times into a single predictive power measure; they are considered as good accuracy measures. The statistical parameters (best, worst, mean, median, standard deviation, RE, and RMS) are calculated to investigate the performance of each optimization approach with variation of iterations. Additionally, it's important to perform Wilcoxon test to investigate the validity of the proposed approach. Referring to results given in Table 2, one can get that, the proposed EMSA succeeded in extracting the optimal parameters of TJS based module with an efficiency of 99.6417% and with best statistical parameters compared to others. In order to investigate the significance of the obtained results via the proposed EMSA compared to other approaches, Kruskal Wallis test is performed then Wilcoxon test is investigated. Finally, Holm-Bonferroni correction test is incorporated to get the corrected p-values of the wilcoxon test, the results of three tests are tabulated in Table 2. For Kruskal Wallis test, the approaches of WOA, MSA and EMSA reject the null hypothesis that all samples are from the same distribution at a 1% significance level. Regarding to the Wilcoxon test of the proposed algorithm, at the default 5% significance level, the value $h = 1$ indicates that the test rejects the null hypothesis of zero median. While for WOA, WCA, GA, PSO and hybrid PSOGWO, the results indicate that the test fails to reject the null hypothesis of zero median in the difference at the default 5% significance level. Finally, the corrected values of p are calculated via Holm-Bonferroni correction test, the value of alpha, the probability of one of more null hypotheses rejection in case of all null hypotheses are true, is selected as 0.05. The results confirmed that, the results obtained via both MSA and EMSA are significant. The responses of all the studied algorithms are shown in Fig. 7 which confirmed the preference of the proposed EMSA. The power-voltage curves obtained by GWO, WOA, WCA, MSA, GA, PSO and hybrid PSOGWO for both experimental and calculated model are given in Fig. 8. The importance of curves given in Fig. 8 is to know the divergence level of each approach model to the experimental one and to confirm the validity of the proposed EMSA.

It is essential to investigate the proposed EMSA with operating the TJS based module under different operating conditions. Therefore, the effect of changing solar radiation is investigated with operating the modules at four cases which are 800 W/m^2, 750 W/m^2, 650 W/m^2, 450 W/m^2, and the experimental data at each case is given in Ref. [23]. The experimental and calculated current-voltage

Table 4
MSA, GA, Hybrid PSOGWO and EMSA optimal powers and statistical parameters under different shadow pattern conditions.

Shadow pattern		Case #1, $G = [900,750,450]$				Case #2, $G = [450,1000,650]$			
		MSA	GA	Hybrid PSOGWO	Proposed EMSA	MSA	GA	Hybrid PSOGWO	Proposed EMSA
Experiment MPP (W)		870.9611				824.0524			
Model MPP (W)		856	826.965	824.5413	868	818.7975	794.124	803.8476	823.1475
Error (W)		1.72%	5.05%	5.33%	0.34%	0.64%	3.631%	0.638%	0.11%
Best		0.1958	0.125	0.1013	0.1189	0.13301	0.1408	0.1380	0.091086
Worst		0.2797	0.139	0.1566	0.2810	0.1749	0.1536	0.1578	0.0943
Mean		0.1951	0.129	0.1068	0.1278	0.1320	0.1421	0.1476	0.0919
Median		0.1958	0.127	0.1035	0.1189	0.1330	0.1409	0.1474	0.0943
Std. dev.		0.0316	0.038	0.0106	0.0112	0.0207	0.035	0.043	0.0132
Efficiency		98.28%	94.95%	94.67%	99.66%	99.36%	96.37%	97.55%	99.89%
Kruskal Wallis test	p-value	1.38e-20	1.72e-18	9.058e-19	6.7902e-25	0.9104	0.6701	0.8452	6.9748e-19
Null hypothesis at 1% significance level		Reject	Reject	Reject	Reject	Accept	Accept	Accept	Reject
Wilcoxon test	p-value	5.92e-17	9.3e-11	1.41e-17	1.12e-37	0.5711	0.0067	0.3699	7.71e-21
	h	1.0	1.0	1.0	1.0	0.0	1.0	0.0	1.0
Null hypothesis of zero median		Reject	Reject	Reject	Reject	Accept	Reject	Accept	Reject
Holm-Bonferroni	p-value	2.96e-16	3.72e-10	8.46e-17	8.96e-37	0.7398	0.0201	0.7398	5.40e-20
Correction test	h	true	true	true	true	false	true	false	true
	Significant	✓	✓	✓	✓	×	✓	×	✓

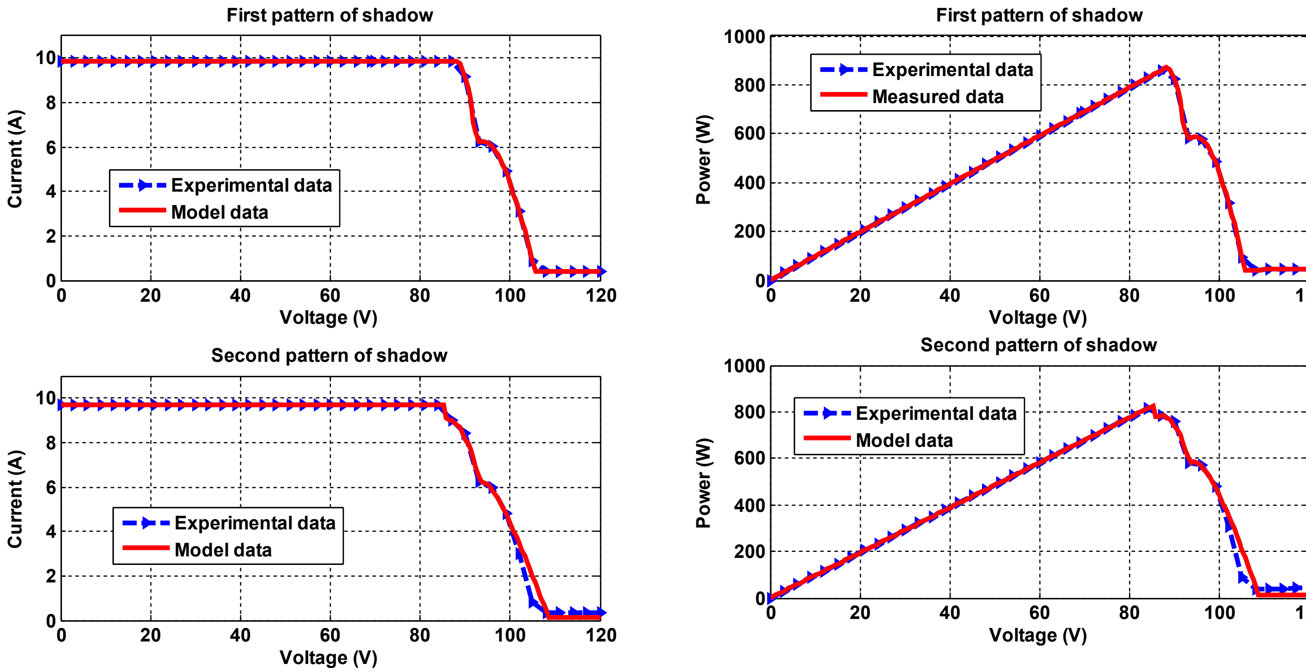

Fig. 13. Experimental and the proposed EMSA model curves under shadow condition.

curves in each case are shown in Fig. 9, both curves are closely matched for all studied cases. Additionally, the power-voltage curves at each solar radiation are given in Fig. 10. The statistical parameters of the proposed EMSA at each studied solar radiation are shown in Table 3, it is clear that the best-obtained error is 0.0081679 A occurs when the module is operated at 450 W/m^2 while the worst error is 0.018565 A occurs for solar radiation of 900 W/m^2. The variation of fitness function obtained via the proposed EMSA with the iteration number at each studied solar radiation is depicted in Fig. 11.

The EMSA succeeded in evaluating the optimal parameters of TJS based module operated under normal distributed solar radiation while what about the occurrence of shadow in existence TJS based array. This question was answered through the application of EMSA on an array consists of three TJS based modules connected in series and built-in Simulink, as shown in Fig. 12(a). The detailed model of each module is given in Fig. 12(b). Two shadow patterns are considered, the first one is [900,750,450] W/m^2 while the second one is [450,1000,650] W/m^2, the first shadow pattern produces 870.96 W maximum experimental power from the array

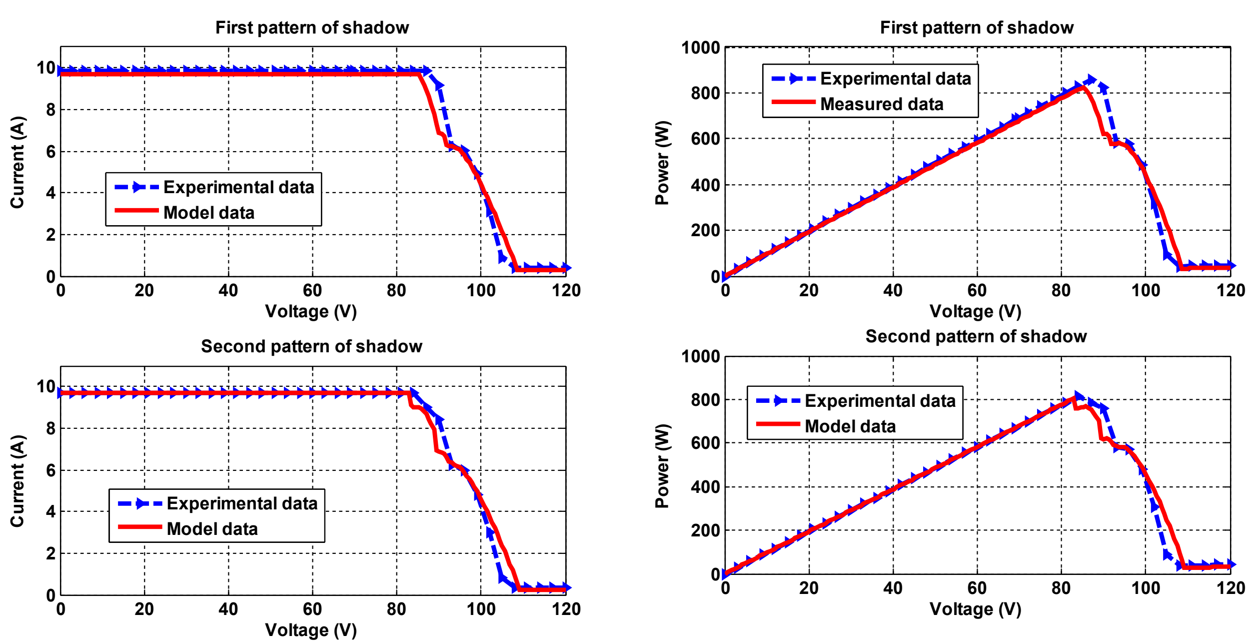

Fig. 14. Experimental and Hybrid PSOGWO model curves under shadow condition.

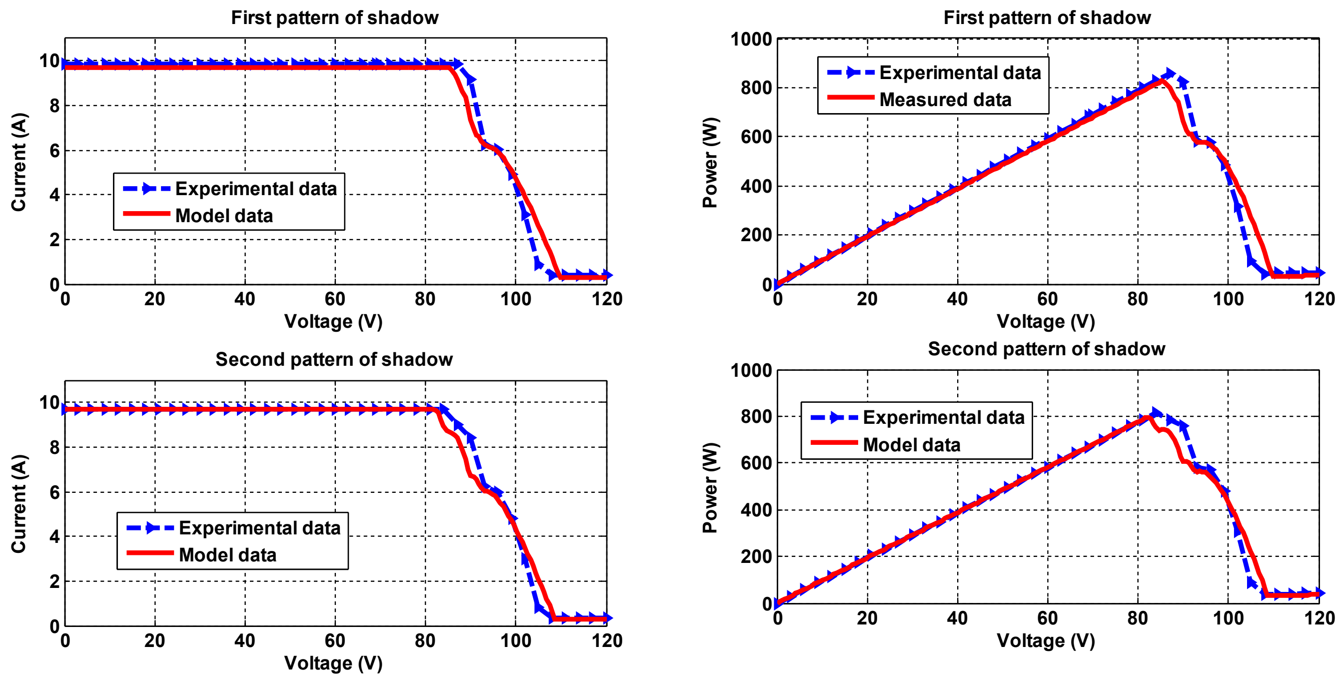

Fig. 15. Experimental and GA model curves under shadow condition.

while the proposed EMSA gives 868 W which is better than the other obtained via MSA, 856 W, this results in an efficiency of 99.66% for EMSA. MSA, GA, Hybrid PSOGWO and EMSA optimal powers and statistical parameters under different shadow pattern conditions are tabulated in Table 4, including the Kruskal Wallis test, Wilcoxon test and Holm-Bonferroni correction test. The proposed EMSA rejects Null hypothesis at 1% significance level for both studied shadow patterns. Regarding the Wilcoxon test, the proposed hybrid approach gives 5% significance level and h = 1, this means the test rejects the null hypothesis of zero median. Additionally, regarding to the Holm-Bonferroni correction test; the proposed EMSA gives significant solution for the two shadow patterns. Referring to the second shadow pattern, the maximum experimental power in such case is 824.0524 W while the EMSA model gives 823.1475 W with an efficiency of 99.89% better than the others. Additionally, the statistical parameters of EMSA are better than those obtained via other approaches in both shadow patterns. The experimental and calculated model curves obtained

Table 6
Comparison between the proposed EMSA ans Hammerstein and wiener optimal parameters.

Parameter	Proposed EMSA	Hammerstein and wiener
A_1	1.9917	1.7552
A_2	1.9220	2.10283
A_3	1.9788	1.8835
R_s (Ω)	0.0206	0.0241
I_{o1} (A)	2.9896e-14	3.0676e-14
I_{o2} (A)	2.56539e-11	1.368e-11
I_{o3} (A)	6.1750	8.2267
I_{L1} (A)	0.0139	0.01435
I_{L2} (A)	0.0149	0.01556
I_{L3} (A)	0.0202	0.0286

Table 5
Hammerstein and wiener identification technique results for different operating conditions.

	At STC (G = 1000 W/m2 and T = 298 K)	Shadow pattern (case #1)	Shadow pattern (case #2)
Input sequence	Pseudo random binary sequence		
Input nonlinearity	Absent		
Output nonlinearity	Polynomial		
No. of samples	121	201	201
Sample time	0.1 s.		
System without noise			
Fit to estimation data	55.64%	63.76%	65.39%
FPE	2.801	1.57	1.385
MSE	2.627	1.51	1.332
System with 20/50 dB SNR noise			
Fit to estimation data	42.74%	68.13%	66.45%
FPE	4.74	1.226	1.314
MSE	4.379	1.168	1.252

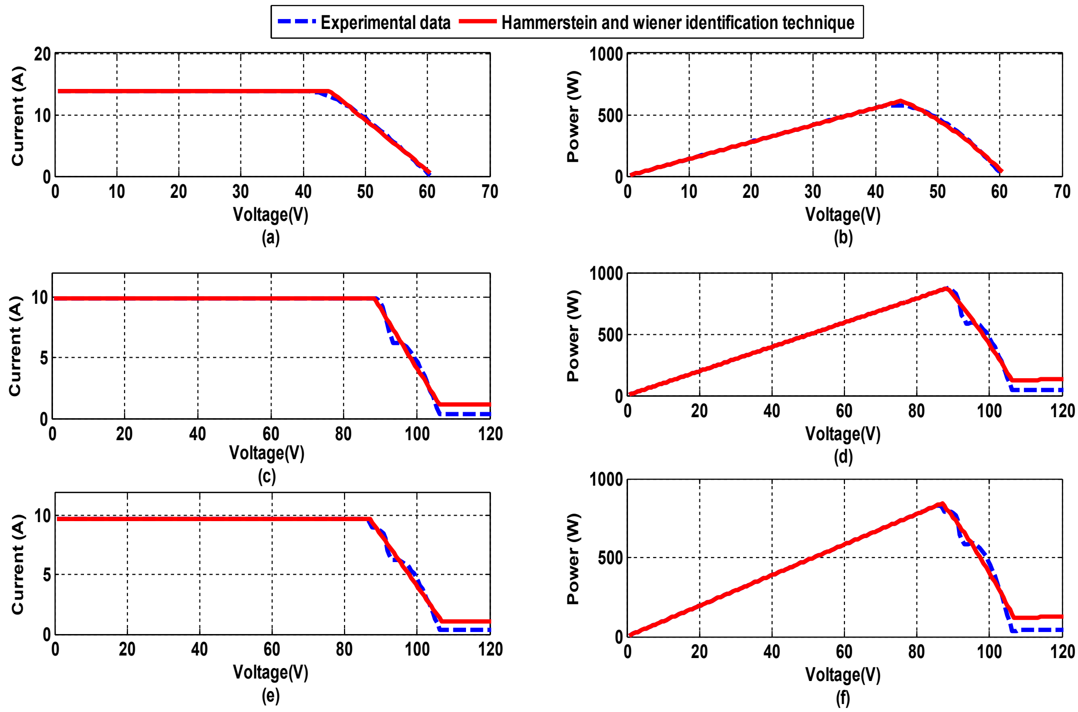

Fig. 16. Experimental and Hammerstein and wiener identification technique model curves without noise, (a) Current-voltage curve at STC, (b) Power-voltage curve at STC, (c) Current-voltage curve at first shadow pattern, (d) Power-voltage curve at first shadow pattern, (e) Current-voltage curve at second shadow pattern, (f) Power-voltage curve at second shadow pattern.

via the proposed EMSA, hybrid POSGWO and GA are given in Fig. 13, Fig. 14, and Fig. 15 respectively.

It is important to investigate the validity of the proposed approach by comparing the obtained results with a well-known Hammerstein and wiener identification technique [35]. This technique represents the dynamic model of a system via linear block sandwiched with two nonlinear blocks. Three operating conditions are considered, STC operation, and the two shadow patterns applied on the array, the sampling time is selected as 0.1 s, the input and output nonlinearities are absent and polynomial respectively, it is assumed that there no noise applied to the system The obtained results are tabulated in Table 5; the best fit to estimation data is

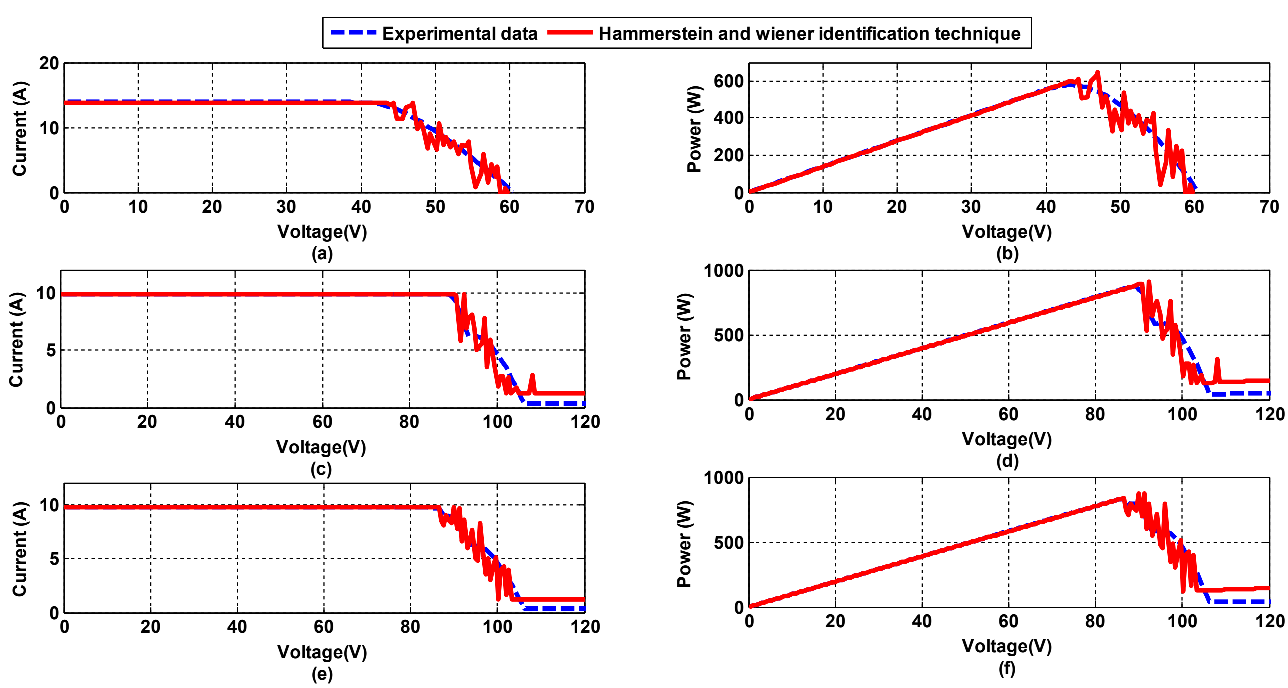

Fig. 17. Experimental and Hammerstein and wiener identification technique model curves with 20/50 dB SNR noise, (a) Current-voltage curve at STC, (b) Power-voltage curve at STC, (c) Current-voltage curve at first shadow pattern, (d) Power-voltage curve at first shadow pattern, (e) Current-voltage curve at second shadow pattern, (f) Power-voltage curve at second shadow pattern.

65.39% occurs in the second shadow pattern; this value confirmed the divergence of the obtained model to the experimental data. Additionally, the best final prediction error (FPE) is 1.385 obtained in the second shadow pattern with the best mean square error (MSE) of 1.332. The optimal estimated parameters obtained via the proposed EMSA and those obtained by Hammerstein and wiener model are tabulated in Table 6. However, the obtained results show the superiority of the proposed EMSA compared to Hammerstein and wiener identification technique as the later failed in obtaining a reliable model converged to the experimental one this is shown via curves obtained in Fig. 16. Additionally, to investigate the robustness of the obtained optimal parameters; 20/50 dB SNR is applied and Hammerstein and wiener identification technique is applied, the results are tabulated in Table 5. It's clear that, the obtained FPE and MSE obtained for the three studied cases are accepted as their values are very close to those obtained from the system without noise, this confirmed the robustness of the obtained optimal parameters of TJS based module obtained via the proposed approach. Fig. 17 shows the curves obtained in case operation under 20/50 dB SNR.

Finally, one can get that; the obtained results confirmed the superiority and reliability of the proposed EMSA in extracting the optimal parameters of TJS based module and array operated at different operating conditions.

7. Conclusion and future works

This work is intended to extract the optimal parameters of Triple-Junction solar-based PV module via the proposed enhanced moth search algorithm (EMSA). The proposed approach incorporates disruptor operator in the traditional moth search algorithm to improve the diversity of MSA and avoiding it from falling in local optima. Integral time absolute error (ITAE) between the module experimental and calculated currents is selected as the objective function. Different operating conditions for TJS based module are analyzed, in addition to the shadow conditions occur in the array. Different heuristic optimization approaches are performed like grey wolf optimizer (GWO), the whale optimization algorithm (WOA), water cycle algorithm (WCA), traditional moth search algorithm (MSA), genetic algorithm (GA), particle swarm optimization (PSO) and hybrid PSOGWO, in addition to comparison with Hammerstein and wiener identification technique is performed, in case of operating TJS based module at STC, the proposed EMSA gives ITAE of 0.014261 A with efficiency 99.6417% while the traditional MSA gives with efficiency 99.16% with fitness function of 0.017209 A. Two shadow patterns are studied on array composing three modules in series, in the first one, the proposed EMSA operates with efficiency of 99.66% while in the second one its efficiency is 99.89%. The results confirmed the superiority of EMSA compared to the others in evaluating the optimal parameters of Triple-Junction solar panel under different operating conditions.

References

[1] Bana S, Saini R. Experimental investigation on power output of different photovoltaic array configurations under uniform and partial shading scenarios. Energy 2017;127:438–53.
[2] Ram JP, Rajasekar N. A new global maximum power point tracking technique for solar photovoltaic (PV) system under partial shading conditions (PSC). Energy 2016;30:1e14.
[3] Mellit A, Kalogirou SA. MPPT-based artificial intelligence techniques for photovoltaic systems and its implementation into field programmable gate array chips: review of current status and future perspectives. Energy 2014;70:1–21.
[4] Rezk H, El-Sayed AHM. Sizing of a stand alone concentrated photovoltaic system in Egyptian site. Int J Electr Power Energy Syst 2013;45(1):325–30.
[5] Green MA, Emery K, Hishikawa Y, Warta W, Dunlop ED. Solar cell efficiency tables (version 48). Prog Photovolt Res Appl 2016;7(24):905–13.
[6] Kinsey GS, Hebert P, Barbour KE, Krut DD, Cotal HL, Sherif RA. Concentrator multijunction solar cell characteristics under variable intensity and temperature. Prog Photovolt Res Appl 2008;16(6):503–8.
[7] Reinhardt KC, Mayberry CS, Lewis BP, Kreifels TL. Multijunction solar cell iso-junction dark current study. Conference Multijunction solar cell iso-junction dark current study. IEEE, p. 1118-1121..
[8] Nishioka K, Takamoto T, Agui T, Kaneiwa M, Uraoka Y, Fuyuki T. Evaluation of InGaP/InGaAs/Ge triple-junction solar cell under concentrated light by simulation program with integrated circuit emphasis. Jpn J Appl Phys 2004;43(3R):882.
[9] Kribus A, Mittelman G. Practical cogeneration with concentrating PV. Conference Practical cogeneration with concentrating PV.
[10] Nishioka K, Takamoto T, Agui T, Kaneiwa M, Uraoka Y, Fuyuki T. Evaluation of temperature characteristics of high-efficiency InGaP/InGaAs/Ge triple-junction solar cells under concentration. Sol Energy Mater Sol Cells 2005;85(3):429–36.
[11] Segev G, Mittelman G, Kribus A. Equivalent circuit models for triple-junction concentrator solar cells. Sol Energy Mater Sol Cells 2012;98:57–65.
[12] Das N, Wongsodihardjo H, Islam S. Modeling of multi-junction photovoltaic cell using MATLAB/Simulink to improve the conversion efficiency. Renew Energy 2015;74:917–24.
[13] Elbaset AA, Ali H, El Sattar MA. New seven parameters model for amorphous silicon and thin film PV modules based on solar irradiance. Sol Energy 2016;138:26–35.
[14] Elbaset AA, Ali H, Abd-El Sattar M. Novel seven-parameter model for photovoltaic modules. Sol Energy Mater Sol Cells 2014;130:442–55.
[15] Patra JC, Maskell DL. Modeling of multi-junction solar cells for estimation of EQE under influence of charged particles using artificial neural networks. Renew Energy 2012;44:7–16.
[16] Chen X, Yu K, Du W, Zhao W, Liu G. Parameters identification of solar cell models using generalized oppositional teaching learning based optimization. Energy 2016;99:170–80.
[17] Askarzadeh A, Rezazadeh A. Parameter identification for solar cell models using harmony search-based algorithms. Sol Energy 2012;86(11):3241–9.
[18] Dkhichi F, Oukarfi B, Fakkar A, Belbounaguia N. Parameter identification of solar cell model using Levenberg–Marquardt algorithm combined with simulated annealing. Sol Energy 2014;110:781–8.
[19] Guo L, Meng Z, Sun Y, Wang L. Parameter identification and sensitivity analysis of solar cell models with cat swarm optimization algorithm. Energy Convers Manag 2016;108:520–8.
[20] Oliva D, Abd El Aziz M, Ella Hassanien A. Parameter estimation of photovoltaic cells using an improved chaotic whale optimization algorithm. Appl Energy 2017;200:141–54.
[21] Gong W, Cai Z. Parameter extraction of solar cell models using repaired adaptive differential evolution. Sol Energy 2013;94:209–20.
[22] AlHajri M, El-Naggar K, AlRashidi M, Al-Othman A. Optimal extraction of solar cell parameters using pattern search. Renew Energy 2012;44:238–45.
[23] Oliva D, Ewees AA, Aziz MAE, Hassanien AE, Peréz-Cisneros M. A chaotic improved artificial bee colony for parameter estimation of photovoltaic cells. Energies 2017;10(7):865.
[24] Wei H, Cong J, Lingyun X, Deyun S. Extracting solar cell model parameters based on chaos particle swarm algorithm. Conference Extracting solar cell model parameters based on chaos particle swarm algorithm. IEEE, p. 398-402..
[25] Zagrouba M, Sellami A, Bouaïcha M, Ksouri M. Identification of PV solar cells and modules parameters using the genetic algorithms: application to maximum power extraction. Sol Energy 2010;84(5):860–6.
[26] Ismail MS, Moghavvemi M, Mahlia T. Characterization of PV panel and global optimization of its model parameters using genetic algorithm. Energy Convers Manag 2013;73:10–25.
[27] Yu K, Qu B, Yue C, Ge S, Chen X, Liang J. A performance-guided JAYA algorithm for parameters identification of photovoltaic cell and module. Appl Energy 2019;237:241–57.
[28] Fathy A, Rezk H. Parameter estimation of photovoltaic system using imperialist competitive algorithm. Renew Energy 2017;111:307–20.
[29] Rezk H, Fathy A. A novel optimal parameters identification of triple-junction solar cell based on a recently meta-heuristic water cycle algorithm. Sol Energy 2017;157:778–91.
[30] Nishioka K, Takamoto T, Agui T, Kaneiwa M, Uraoka Y, Fuyuki T. Evaluation of InGaP/InGaAs/Ge triple-junction solar cell and optimization of solar cell's structure focusing on series resistance for high-efficiency concentrator photovoltaic systems. Sol Energy Mater Sol Cells 2006;90(9):1308–21.
[31] Tsai H-L, Tu C-S, Su Y-J. Development of generalized photovoltaic model using MATLAB/SIMULINK. Conference Development of generalized photovoltaic model using MATLAB/SIMULINK, vol. 2008. San Francisco, USA, p. 1-6.
[32] Wang G-G. Moth search algorithm: a bio-inspired metaheuristic algorithm for global optimization problems. Memet. Comput. 2016:1–14.
[33] Feng Y, Wang G-G. Binary moth search algorithm for discounted 0-1 knapsack problem. IEEE Access 2018;6:10708–19.
[34] Bansal JC, Farswan P. A novel disruption in biogeography-based optimization with application to optimal power flow problem. Appl Intell 2017;46(3):590–615.
[35] Wills A, Schön TB, Ljung L. Ninness B identification of hammerstein–wiener models. Automatica 2013;49(1):70–81.